Iraqi Journal of Biotechnology, 2026, Vol. 25, No. 1, 215-227.

Evaluation of The Biological Effect of synthesized Iron Oxide NPs against *Acinetobacter baumannii*

[1]Ansar R. Mansor, [2] Laith Ahmad Yaaqoob

[1,2]Biotechnology Department, Collage of Science, University of Baghdad

Received: October 20, 2024 / Accepted: November 10, 2024 / Published: March 30, 2026

Abstract

Background. *Acinetobacter baumannii* is a multidrug-resistant pathogen responsible for severe hospital-acquired infections. The increasing resistance to conventional antibiotics has directed attention toward green nanotechnology. **Aim.** This study aimed to biosynthesize iron oxide (Fe_2O_3) nanoparticles using pyocyanin pigment from *Pseudomonas aeruginosa* and evaluate their antibacterial activity against *A. baumannii*. **Methods.** *A. baumannii* were identified using VITEK-2 and standard biochemical tests. Pyocyanin pigment was extracted for Fe_2O_3 nanoparticle synthesis. The synthesized nanoparticles were characterized using UV–Vis spectroscopy, AFM, FTIR, and FE-SEM, while antibacterial activity was assessed by the agar well diffusion method. **Results.** UV–Vis analysis confirmed nanoparticle formation with characteristic absorption peaks. AFM and FE-SEM revealed nanoscale particles with an average size of approximately 35 nm and rod-shaped morphology. FTIR analysis indicated the presence of functional groups responsible for nanoparticle stabilization. Antibacterial assays demonstrated concentration-dependent inhibitory activity against *A. baumannii*, with the highest inhibition zone observed at 50 µg/mL of iron oxide nanoparticles. **Conclusion.** The synthesized nanoparticles exhibited notable antibacterial activity against multidrug-resistant *A. baumannii*.

Keywords: Biological pigment, Biosynthesis NPs, Antimicrobial activity, Fe_2O_3 NPs.

Corresponding author: anssar.raheem2306@sc.uobaghdad.edu.iq ,laith.yaaqoob@sc.uobaghdad.edu.iq

Introduction

Acinetobacter baumannii is a type of bacteria that is named after the American bacteriologists Paul and Linda Baumann. It is a Gram-negative bacterium that does not have the ability to move, and it has a shape that is between a sphere and a rod, with a size ranging from 1 to 1.5 micrometres (1). It is commonly found in pairs or long chains, and its length can vary, especially during the stationary phase. As it matures, it tends to become more spherical in shape. *Acinetobacter baumannii* is a multidrug-resistant pathogen, meaning it is resistant to multiple types of drugs. In hospitals and other healthcare facilities, it may lead to infections, especially in critically ill patients or those with compromised immune systems who have central venous catheters. and caused serious to patients with burn and wound infections (2). *A. baumannii* has acquired a wide range of resistance to antimicrobial agents, which is linked to a higher death rate in infected individuals compared to other species that are not *A. baumannii. A. baumannii* is capable of causing many infections, with the respiratory tract being the most commonly affected, particularly in cases of ventilator-associated pneumonia. Instances of meningitis linked to *A. baumannii* have been recorded. The primary factor of risk

for acquiring multidrug-resistant (MDR) infections is factors contributing to the presence of *A. baumannii* include prior antibiotic usage, subsequent mechanical breathing, duration of ICU/hospitalization, severity of disease, and utilization of medical devices (1, 3) NPs and nano-biomedicine involve the ability to measure, display, control, and create objects at an atomic level, typically ranging from 1 to 100 nanometers. In today's world, the efficiency and size reduction of electronic devices are crucial factors, with nanomaterials playing a significant part in achieving these goals. Nanotechnology is attracting widespread attention due to its extensive range of applications across various industries, including textiles and medicine. One particularly important aspect is its use as an antibacterial agent. Nanostructures are widely employed in fields such as engineering, medicine, environmental remediation, biotechnology, microbiology, electronics, optics, mechanics and material sciences (4,5). The utilization of ecologically friendly raw materials, such as biological extracts derived from bacteria, for the production of NPs of iron oxide offers numerous compatible and economic benefits. Drug firms and therapeutic targets benefit from the prevention of using harmful chemicals in the manufacturing technique. (4,6). Chemical synthesis procedures introduce hazardous compounds that may have detrimental impacts in medical applications. Bacteria are currently being utilized to biologically synthesise metallic NPs, and their extracts are being utilised for scientific purposes. (7,8,9). Biological systems, like bacteria, consist of macromolecules, the majority of which are within the nanoscale scale (8). The process of extracting cells from these species of bacteria is utilised to generate NPs with biological components and diverse sizes (8). The isolated bacteria include components that are responsible for iron reduction. Ferric sulphate and other suitable substrates can be utilised to diminish bacterial extracts. (10) (9). Biological nanotechnology is a highly intriguing field that encompasses a diverse range of techniques aimed at reducing or eliminating hazardous chemicals. to the conservation of the environment. Biological manufacturing offers greater benefits compared to chemical and physical approaches due to its simplicity in processing, cost-effectiveness, and scalability for large-scale production. (11,12). Magnetic iron oxide NPs are the preferred choice for biological and medical specialised applications because of their chemical stability, superparamagnetic behaviour, and biocompatibility (13). The production of iron NPs (Fe_2O_3) NPS utilising bacterial and fungal extracts has notable advantages compared to chemical and physical methods due to its simplicity in handling, cost-effectiveness, and ability to be scaled up for mass production. This technique did not require the utilisation of expensive high-pressure apparatus, hazardous chemicals or elevated temperatures. The pigment was determined to be produced by Gram-negative *P. aeruginosa* (14). One of the distinctive features of *Pseudomonas aeruginosa* is its capacity to synthesise the blue-green pigment pyocyanin. This study was aimed; the purified pyocyanin from *P. aeruginosa* was used to biosynthesize iron oxide nanoparticles as a reducing and stabilizing agent. As well as the potential application of the synthesized

nanoparticles in vitro as an antibacterial activity against *A. baumannii*.

Materials and methods

The isolated bacteria *Acinetobacter baumannii* were collected from December 2023 to April 2024, this encompasses A total of 120 samples The Vitek-2 system and standard biochemical test were utilized to identify all bacterial isolates. The antimicrobial efficacy and other characteristics of Iron oxide NPs were investigated using multidrug-resistant *A. baumannii* strains. (15, 16)

Bacterial isolation identification VITEK 2 system

This process has multiple stages, including:

A single, intact colony was placed into a test tube containing normal saline (3mL). An automated densities check verified that the concentration of the colony adhered to McFarland's recommended value of 1.5 x 10^8 CFU/ml. The computer software could utilise the barcode on the cassette to accurately identify the sample once standardised inoculums were introduced. Once the barcode is scanned, a VITEK 2 card type becomes linked to a sample ID number.

Identification by biochemical tests

1. **Indole test:** Peptone broth medium was utilised for inoculation of cultures of bacteria, which were then cultured at 37 degrees Celsius for 18 to 24 hours. A positive indicator for the experiment was the appearance of a crimson ring upon addition of Kovac's reagent to each tube.
2. **Oxidase test:** An aseptic wooden rod was employed to gently apply a sample of the tested bacterial culture onto the filter paper that had been soaked in oxidase solution(17). A favourable result was determined if the colony rapidly changed colour to ink blue(18).
3. **Simmons Citrate:** Following 48 to 72 hours of incubation at 37°C, the bacterial culture was transferred on a Simmons citrate slant. A change from green to blue in the test findings indicates a favorable outcome (19).
4. **Urease test:** The urea agar slant was placed in an incubator set at 37°C, together with a freshly obtained bacterial culture. After twenty-four the results of the examination were announced. The transition from white to purple-pink in the medium's colouration indicates a successful conclusion (19).
5. **Catalase production test:** A glass slide was coated with a modest quantity of hydrogen peroxide (3 percent H_2O_2), and a loop containing previously confirmed bacterial cultures was agitated with the peroxide. The test was deemed positive if bubbles formed.

Pyocyanin pigment production

After collecting each *P. aeruginosa* isolate sample, they were inoculated into Luria Broth medium (20) and placed in an incubator at a temperature of 28˚C for a period of 120 hours. Subsequently, the samples were subjected to analysis. Upon agitation of the flask, the green pigment of pyocyanin was evenly dispersed through the whole broth, resulting in a blue-green coloration of the medium (Figure 3). Based on (14), A 250 ml sample of a broth culture of *P. aeruginosa* was obtained after incubation. The liquid was then subjected to centrifugation for a duration of 15 minutes at a speed of 8000 revolutions per minute. As a result, a supernatant and a deposit were formed. The deposit was disregarded. In order to obtain pyocyanin, chloroform has been introduced to precipitate and produce

pyocyanin (21). The pyocyanin was extracted using a rotary evaporator and lyophilized pyocyanin by using a vacuum freeze dryer, resulting in the collection of pyocyanin powder.

Biosynthesis of Iron Nano particles.

The initial step in utilising pyocyanin for the biosynthesis of iron (Fe_2O_3) NPs involves synthesising the compound. This is achieved by combining of deionized distilled water (DDW) (50ml) and pyocyanin powder (5mg) and dispersing it using an ultrasonication bath for a duration of 30 minutes. Additionally, (5g) of iron oxide is dispersed in 50 ml of pyocyanin, which was previously prepared in a flask and agitated overnight in a darkroom. Subsequently, the concoction underwent centrifugation at a speed of 8000 revolutions per minute for a duration of 10 minutes. The solution containing the whole iron (Fe_2O_3) NPs was subjected to two rounds of washing with deionized distilled water to eliminate any residual pyocyanin pigment. The NPs were dried by subjecting them to an oven at a temperature of 37°C for the duration of one night. Ultimately, the black material was enclosed within an opaque vessel to hinder its evaporation (22).

Antibacterial activity of iron (Fe_2O_3) NPs

The bacterial susceptibility to iron (Fe_2O_3) NPs was evaluated using the agar well diffusion method. The Mueller Hinton medium was utilised in this examination. *Acinetobacter baumannii* was cultured for 24 hours at a temperature of 37°C. Following the incubation period, a standard inoculum was prepared for each bacterial isolate. The concentration of the inoculum was 1.5 X 10^8 CFU / mL, as per the standard 0.5 McFarland solution. Aseptic technique was utilized to immerse a small sterile brush into the tube containing the bacterial suspension. The swab was then utilized to evenly spread the bacteria onto the surface of a Muller Hinton agar (MH) plate. On MH agar plates, aseptic preparation of wells with a 6 mm diameter was carried out. Subsequently, 1 mL of Fe_2O_3 NPs at various concentrations (50,25, 12.5, 6.25, 3.125, and 1.5625 µg/ml) were distributed into individual wells. The plates were then incubated overnight at 37°C. After the period of incubation, the widths of the zones indicating the susceptibility of the bacteria were measured and documented (22, 23).

Results

VITEK 2 compact system

Figure 1 illustrate result of *A. baumannii* VITEK2 system.

bioMérieux Customer: Microbiology Chart Report Printed April 30, 2024 1:46:20 PM AST

Patient Name: B 19, . Patient ID: sgtwe
Location: Physician:
Lab ID: 5 Isolate Number: 1

Organism Quantity:
Selected Organism : Acinetobacter baumannii complex

Source: **Collected:**

Comments:	

Identification Information	**Analysis Time:**	5.80 hours	**Status:**	Final
Selected Organism	99% Probability **Bionumber:**	**Acinetobacter baumannii complex** 0241010103500210		
ID Analysis Messages				

Biochemical Details

2	APPA	-	3	ADO	-	4	PyrA	-	5	lARL	-	7	dCEL	+	9	BGAL	-
10	H2S	-	11	BNAG	-	12	AGLTp	+	13	dGLU	+	14	GGT	-	15	OFF	-
17	BGLU	-	18	dMAL	-	19	dMAN	-	20	dMNE	+	21	BXYL	-	22	BAlap	-
23	ProA	-	26	LIP	-	27	PLE	-	29	TyrA	+	31	URE	-	32	dSOR	-
33	SAC	-	34	dTAG	-	35	dTRE	-	36	CIT	+	37	MNT	+	39	5KG	-
40	lLATk	+	41	AGLU	-	42	SUCT	+	43	NAGA	-	44	AGAL	-	45	PHOS	-
46	GlyA	-	47	ODC	-	48	LDC	-	53	lHISa	-	56	CMT	+	57	BGUR	-
58	O129R	+	59	GGAA	-	61	lMLTa	-	62	ELLM	-	64	lLATa	-			

Figure (1): VITEK II system for *Acinetobacter baumannii*.

Biochemical test

Figure 2 and Table 1 displayed the results of the biochemical test conducted on *A. baumannii*.

Table (1): The result of the biochemical test.

Test	results
Indole test	-
Oxidase test	-
Simmons Citrate test	+
Urase test	-
Catalase test	+

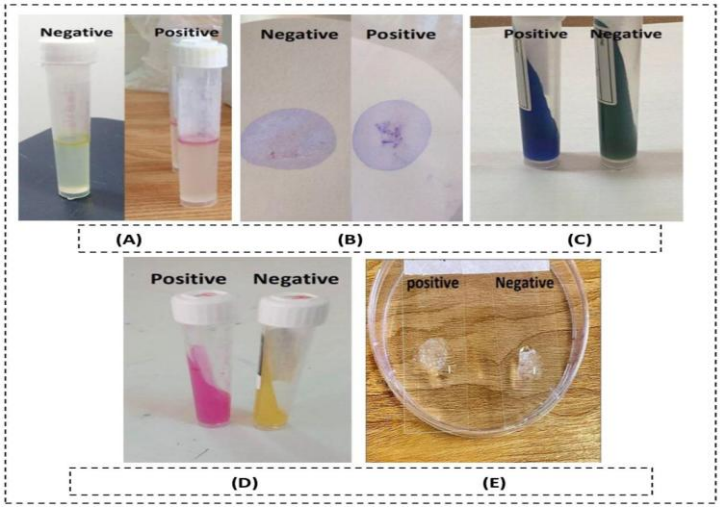

Figure (2): Biochemical tests for identification of bacterial isolate, (A): Indole test, (B): Oxidase test, (C): Simmons Citrate test, (D): Urease test, (E): Catalase test.

Pyocyanin pigment extraction

As the flask was agitated, the green pigment that had settled on the broth's surface washed into and distributed throughout the liquid (Figure 3).

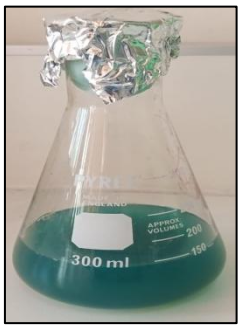

Figure (3): The Extracted pyocyanin

Characterization of Pyocyanin pigment

The UV–VIS spectral analysis of Pyocyanin

The pyocyanin developed by *P. aeruginosa* is characterized by scanning a UV-visible spectrophotometer in figure 4 to detect the maximum absorption at 363 nm.

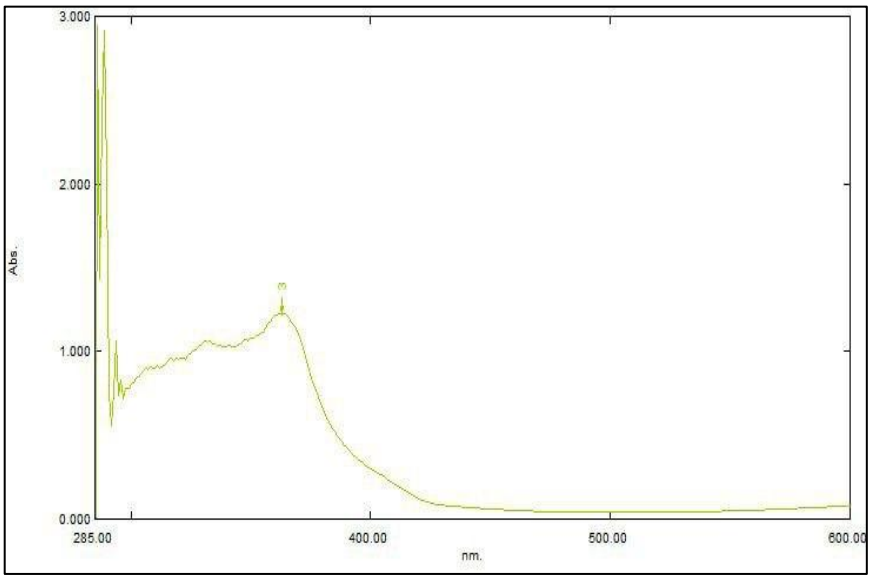

Figure (4): UV-VIS of pyocyanin.

UV–VIS spectral analysis of iron (Fe_2O_3) NPs

Figure 5 shows the results of scanning a UV-visible spectrophotometer for maximum absorption; the iron NPs were found to have an absorbance at 290 nm.

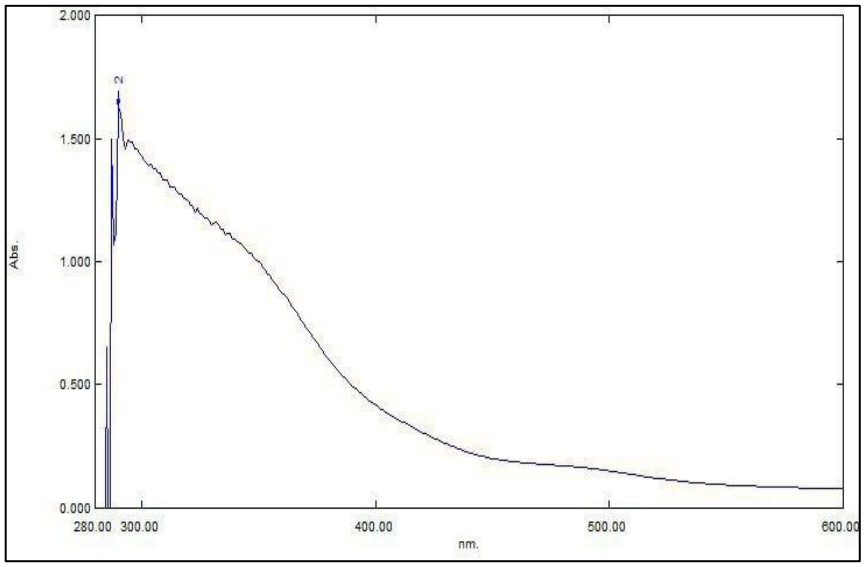

Figure (5): UV-VIS of Fe_2O_3 NPs.

Atomic Force Microscope (AFM) of Iron Nano particles.

The formation of (Fe_2O_3) surface shape of the NPs was examined via atomic force microscopy to displayed that (Fe_2O_3) NPs was in an average diameter size (Mean) of 35.58nm (Figure 6).

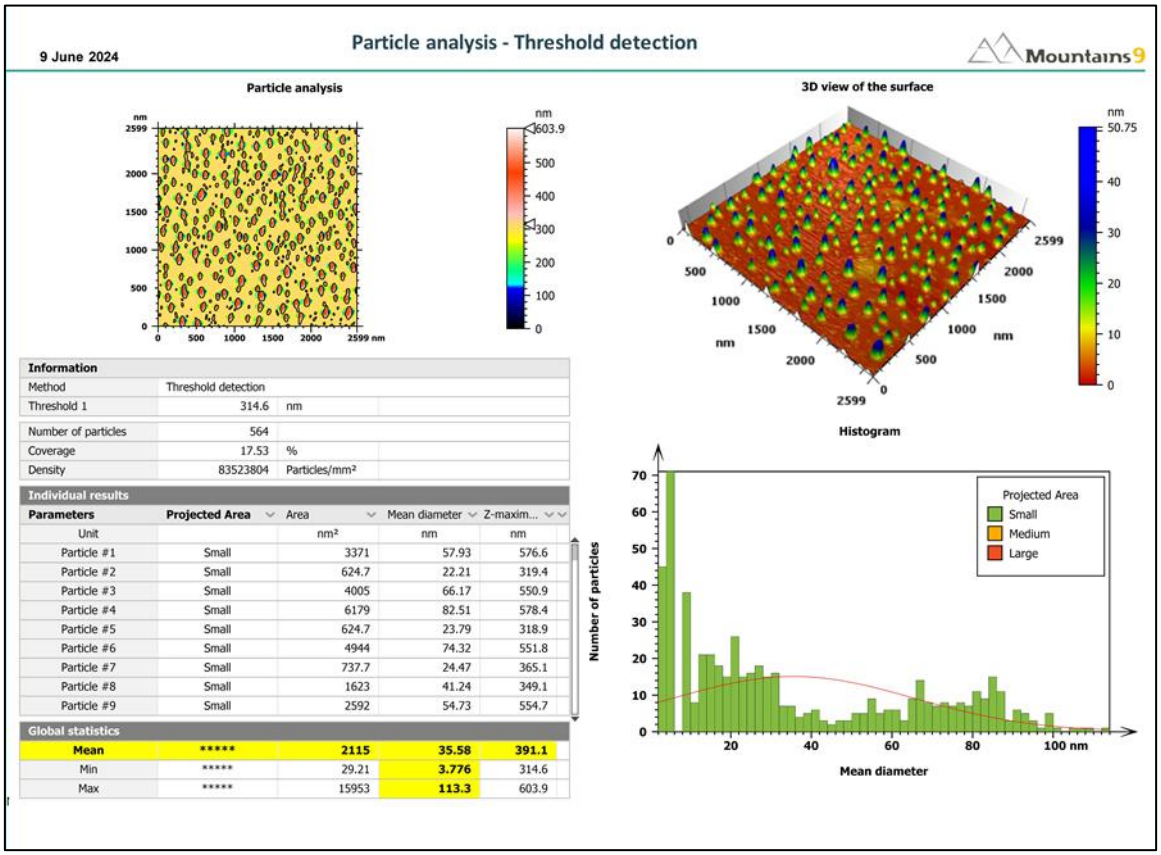

Figure (6): Atomic Force Microscopy of Fe_2O_3 NPs (Histogram of iron oxide NPs, 3D of iron oxide NPs).

Fourier transforms infrared (FTIR) spectroscopy analysis

Figure (7) display the FT-IR data for the iron oxide NPs produced via biosynthesis. Based on the result in table (2), it is common to see a succession of absorption peaks between 4000 and 400 cm^{-1}, which correspond to hydroxyl and carboxylate groups in the substance. In particular, the frequency range of about (680.83- 410.81) cm^{-1}.

Table (2): FTIR of NP of (Fe_2O_3).

Compound	Absorption Frequency (cm^{-1})	Bonds	Functional Groups' Compound class
Pyocyanin Extract	3394.48	N-H stretching	Primary amine
	2873.74-2800.45	O-H bending	Alcohol
	2615.29	C-H Stretching	Aldehyde
	1654.81	C=C stretching	Alkene
	1550.66-1488.94	N-O stretching	Nitro compound
	1461.94-1398.30	C-H bending	Alkene
	1118.64-1074.28	C-N stretching	Amine
	617.18	C-Br stretching	Halo compound
	794.62-765.69	C=C bending	Alkene
Ferric Sulfate	3394.48-3371.34	N-H stretching	Primary amine
	1614.31	C=C stretching	Alkene
	684.68	Metal Oxide	Fe_2O_3
	414.67	Metal Oxide	Fe_2O_3
Fe_2O_3 (NPs)	3386.77-3369.41	N-H stretching	primary amine
	2437.86-2324.06	O=C=O stretching	Carbon dioxide
	1614.31	C=C stretching	Alkene
	680.83	Metal Oxide	Fe_2O_3
	428.17-410.81	Metal Oxide	Fe_2O_3

Field emission scanning electron microscopy (FE-SEM) analysis

Analyzing the biosynthesized iron oxide NPs' morphological characteristics was done using the field-effect scanning electron microscopy technique. Figure 8 shows that the sample included the synthetic iron oxide NPs with rod shaped and the size of iron oxide NPs in average diameter (31.99-21.98) nm.

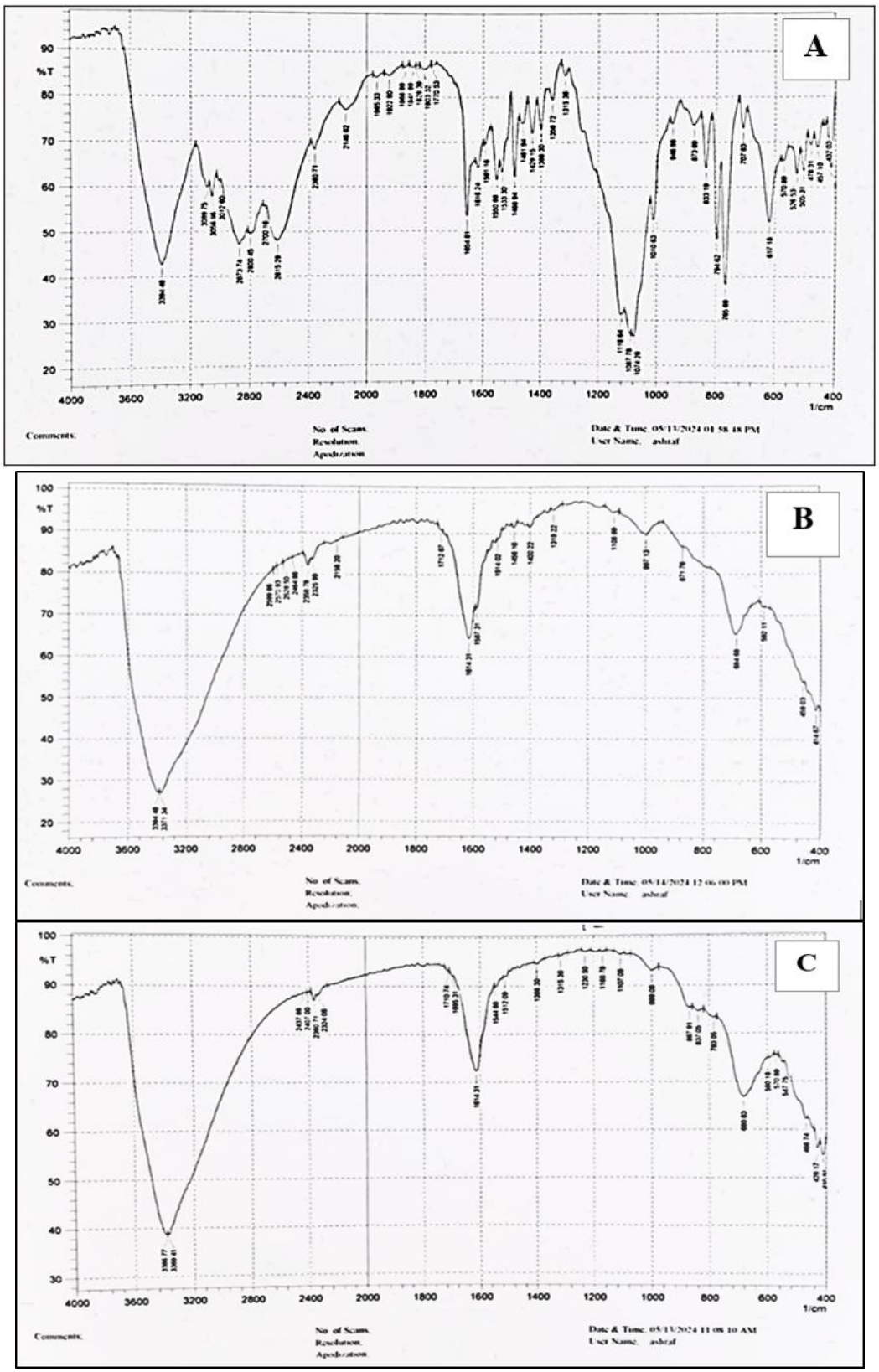

Figure (7): FTIR images of (Fe_2O_3) NPs synthesized using pyocyanin pigment, A: pyocyanin pigment. B: Ferric sulfate. C: (Fe_2O_3)NPs.

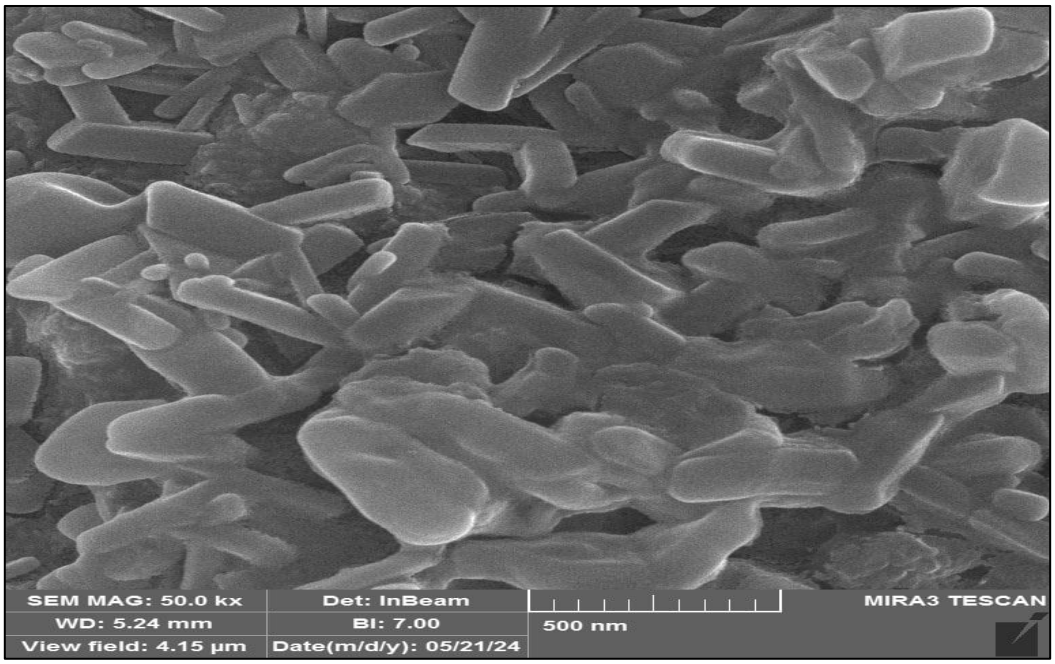

Figure (8): Images of the biosynthesized iron oxide NPs using FE-SEM

Antibacterial Activity of Iron NPs

The antibacterial effect of iron oxide nanoparticles against Acinetobacter baumannii is concentration-dependent, according to the results presented in Table (3). The maximum concentration tested, 50 µg/mL, presented the highest inhibition zone value of 21 mm, relating to strong antibacterial activity. With a decrease in the nanoparticle concentration, there was gradual diminution in the diameter of inhibition zones for the other dilutions tested; their values declined to 18 mm with 25 µg/mL, further to 13 mm with 12.5 µg/mL, and finally to 10 mm for 6.25 µg/mL. At the lower concentrations, no marked evidence in terms of the antibacterial impact was realized, as expressed by the reduced inhibition zone value recorded at 3.125 µg/mL with a value of 5 mm, while at a concentration of 1.5625 µg/mL, no inhibition activity was observed for the nanoparticles. These observations thus point to a relationship between the increase in the antibacterial efficiency of iron oxide nanoparticles with respect to A. baumannii and their concentrations.

Table (3): Antibacterial activity Test of Iron NPs For *A. baumannii*

Iron NPS con.(µg/ml)	ZONE OF Diameter (mm)
50	21
25	18
12.5	13
6.25	10
3.125	5
1.5625	No inhibition Zone

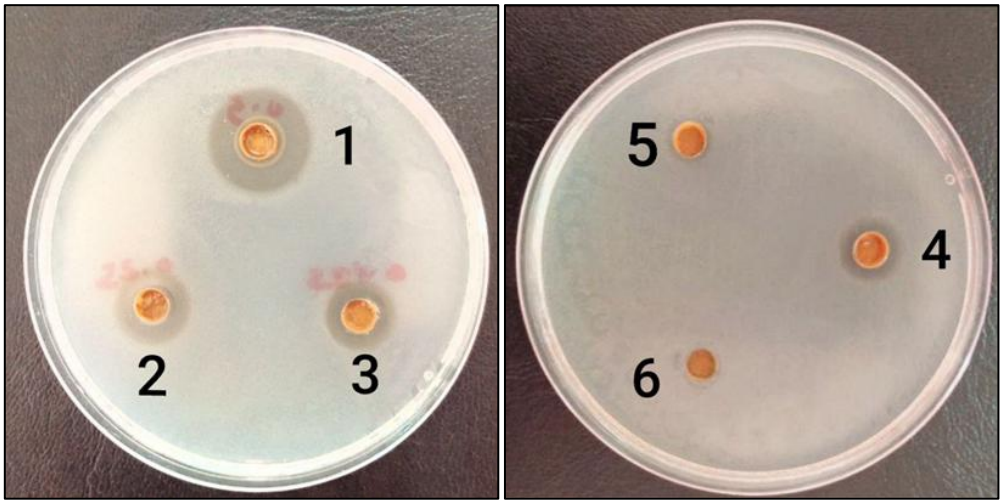

Figure (9): Antibacterial susceptibility test of Iron NPs against *A. baumannii* at different concentrations. 1 : 50; 2 : 25; 3: 12.5; 4 : 6.25; 5 : 3.125; 6: 1.5625.

Discussion

In agreement with this finding of this work about the extraction method of pyocyanin, the study was represented similar results (24). In addition, The pyocyanin was characterized by different approaches, included UV-visible spectrophotometer (25), whereas absorbance was measured at 363 nm in corresponding with the result was shown by (22) that indicates the UV-visible of Fe_2O_3 is 315nm. Using UV-Vis, the iron NPs were found to have an absorbance at 290 nm in corresponding with the result was shown by (26) that indicates the UV-visible of Fe_2O_3 is 304nm. In addition, AFM was showed that an average diameter size (Mean) of 35.58 nm, in corresponding with the result was shown by (27) that indicates the average diameter size (Mean) of Fe_2O_3 is 35.01nm. Also, FTIR indicated that the frequency range of about (680.83- 410.81) cm^{-1} in corresponding with the result was shown by (28) that indicates the FTIR of Fe_2O_3 is (634.54-418.52) cm^{-1}. Using FE-SEM, the synthetic iron oxide NPs with rod shaped and the size of iron oxide NPs was in average diameter (31.99-21.98) nm in corresponding with the result was shown by (27) that indicates the FE-SEM of Fe_2O_3 NPs is (23.43-15.49) nm. Iron NPs was applied as antibacterial agent for MDR- *A. baumannii* with strong biofilm production, whereas its effects depended upon NP's concentration. The main mechanism of Iron NPs toxicity is potentially associated with the nanoparticles interact with bacteria by altering the membrane's shape and increasing permeability. It alters transporting across the plasma membrane, resulting in cell death (28).

Conclusions

1. Green synthesis of iron oxide NPs from pyocyanin was an effective method to give the best properties for NPs synthesized.
2. Iron NPs anti-bacterial against *A. baumannii* bacterial isolates.

References

1. Jung, J. and Park, W. (2015) Acinetobacter species as model microorganisms in environmental microbiology: current state and perspectives. Applied Microbiology and Biotechnology, 99, pp. 2533–2548.
2. AL-falahat, S.Y. and Al-Draghi, W.A. (2022) Molecular detection of rblB and

csgA genes of Acinetobacter baumannii isolated from different clinical and environmental samples. Iraqi Journal of Biotechnology, 21(2), pp. 594–602.
3. Vázquez-López, R., Solano-Gálvez, S.G., Juárez Vignon-Whaley, J.J., Abello Vaamonde, J.A., Padró Alonzo, L.A., Rivera Reséndiz, A. et al. (2020) Acinetobacter baumannii resistance: a real challenge for clinicians. Antibiotics, 9(4), p. 205.
4. Al-Azawi, M.T., Hadi, S. and Mohammed, C.H. (2019) Synthesis of silica nanoparticles via green approach using hot aqueous extract of Thuja orientalis leaf and their effect on biofilm formation. Iraqi Journal of Agricultural Sciences, 50, pp. 1–10.
5. Zhang, L. and Webster, T.J. (2009) Nanotechnology and nanomaterials: promises for improved tissue regeneration. Nano Today, 4(1), pp. 66–80.
6. Christian, P., Von der Kammer, F., Baalousha, M. and Hofmann, T. (2008) Nanoparticles: structure, properties, preparation and behaviour in environmental media. Ecotoxicology, 17, pp. 326–343.
7. Das, A.K., Marwal, A. and Verma, R. (2014) Datura inoxia leaf extract mediated one-step green synthesis and characterization of magnetite (Fe_3O_4) nanoparticles. Research and Reviews: Journal of Pharmaceutics and Nanotechnology, 2(2), pp. 21–24.
8. Edwards, P.R. and Ewing, W.H. (1973) Identification of Enterobacteriaceae. Journal of Hygiene, Epidemiology, Microbiology and Immunology, 17(3), pp. 1–20.
9. Liu, J., Qiao, S.Z., Hu, Q.H. and Lu, G.Q. (2011) Magnetic nanocomposites with mesoporous structures: synthesis and applications. Small, 7(4), pp. 425–443.
10. Forbes, B.A., Sahm, D.F. and Weissfeld, A.S. (2007) Diagnostic Microbiology. St. Louis: Mosby.
11. Fortina, M.G., Ricci, G., Mora, D. and Manachini, P. (2004) Molecular analysis of artisanal Italian cheeses reveals Enterococcus italicus sp. nov. International Journal of Systematic and Evolutionary Microbiology, 54(5), pp. 1717–1721.
12. Shameli, K., Ahmad, M.B., Zamanian, A., Sangpour, P., Shabanzadeh, P., Abdollahi, Y. et al. (2012) Green biosynthesis of silver nanoparticles using Curcuma longa tuber powder. International Journal of Nanomedicine, 7, pp. 5603–5610.
13. Mahdavi, M., Ahmad, M.B., Haron, M.J., Namvar, F., Nadi, B., Rahman, M.Z.A. et al. (2013) Synthesis, surface modification and characterisation of biocompatible magnetic iron oxide nanoparticles for biomedical applications. Molecules, 18(7), pp. 7533–7548.
14. Mirzaei, R., Mohammadzadeh, R., Alikhani, M.Y., Shokri Moghadam, M., Karampoor, S., Kazemi, S. et al. (2020) The biofilm-associated bacterial infections unrelated to indwelling devices. IUBMB Life, 72(7), pp. 1271–1285.
15. Seil, J.T. and Webster, T.J. (2012) Antimicrobial applications of nanotechnology: methods and literature. International Journal of Nanomedicine, 7, pp. 2767–2781.
16. Altaee, M.F., Yaaqoob, L.A. and Kamona, Z.K. (2020) Evaluation of the biological activity of nickel oxide nanoparticles as antibacterial and anticancer agents. Iraqi Journal of Science, 61, pp. 2888–2896.
17. Collee, J.G., Fraser, A.G., Marmion, B.P. and Simmons, A. (1996) Mackie and McCartney Practical Medical Microbiology. 14th edn. New York: Churchill Livingstone.
18. Benson, H.J. (2002) Microbiological Applications: A Laboratory Manual in General Microbiology. New York: McGraw-Hill.
19. MacFaddin, J.F. (2000) Biochemical Tests for Identification of Medical Bacteria. Baltimore: Lippincott Williams and Wilkins.
20. Roy, R., Tiwari, M., Donelli, G. and Tiwari, V. (2018) Strategies for combating bacterial biofilms: a focus on anti-biofilm agents and their mechanisms of action. Virulence, 9(1), pp. 522–554.
21. Yaaqoob, U.R.H., Yaaqoob, L.A. (2022) Antibacterial activity of cobalt and titanium ($Co:TiO_2$) core-shell nanoparticles against Escherichia coli isolated from urinary tract infections. Iraqi Journal of Biotechnology, 21(2), pp. 1–10.
22. Hameed, U. and Yaaqoob, L. (Year not specified) Evaluation of antibacterial activity of cobalt (Co) nanoparticles against Escherichia coli. Unpublished manuscript.

23. Smaill, F. (2000) Antibiotic susceptibility and resistance testing: an overview. Canadian Journal of Gastroenterology and Hepatology, 14, pp. 871–875.
24. Hamza, M. and Yaaqoob, L. (2020) Evaluation of the effect of green synthesis titanium dioxide nanoparticles on Acinetobacter baumannii isolates. Iraqi Journal of Agricultural Sciences, 51(6), pp. 1–10.
25. Schulze, A., Mitterer, F., Pombo, J.P. and Schild, S. (2021) Biofilms by bacterial human pathogens: clinical relevance, development, composition and regulation. Microbial Cell, 8(2), p. 28.
26. Yaaqoob, M.A.Q. and Yaaqoob, L.A. (2022) Effectivity of iron oxide nanoparticles synthesis by intracellular Lactobacillus as an antibacterial agent against Pseudomonas aeruginosa. Iraqi Journal of Biotechnology, 21(2), pp. 1–10.
27. Yaaqoob, L. (2022) Evaluation of the biological effect of synthesized iron oxide nanoparticles on Enterococcus faecalis. Iraqi Journal of Agricultural Sciences, 53(2), pp. 440–452.
28. Li, S.K., Shen, Y.H., Xie, A.J., Yu, X.R., Qiu, L.G., Zhang, L. et al. (2007) Green synthesis of silver nanoparticles using Capsicum annuum L. extract. Journal name not specified, pp. 1–8.